Journal of Non-Crystalline Solids 692 (2026) 124332

Contents lists available at ScienceDirect

Journal of Non-Crystalline Solids

journal homepage: www.elsevier.com/locate/jnoncrysol

Electronic subgap levels due to point and surface defects in silica glass and α-quartz

Wolfgang Körner [a,*], Manuel Enns [a], Peter Gumbsch [a,b], Daniel F. Urban [a,c], Christian Elsässer [a,c]

[a] Fraunhofer Institute for Mechanics of Materials IWM, Wöhlerstraße 11, 79108 Freiburg, Germany
[b] Institute for Applied Materials (IAM), Karlsruhe Institute of Technology (KIT), Kaiserstraße 12, 76131 Karlsruhe, Germany
[c] Freiburg Materials Research Center (FMF), Albert-Ludwigs-Universität, Stefan-Meier-Straße 21, 79104 Freiburg, Germany

ARTICLE INFO

Keywords:
Silica glass
Subgap states
Absorption
DFT
Density of states

ABSTRACT

We present a theoretical study with focus on the transparency of silica glass (a-SiO_2) in the ultraviolet light spectrum. All imperfections in the crystal structure can cause electronic subgap levels and thus increase the absorption of light. Therefore, we investigate a wide variety of defects and their respective electronic levels, like intrinsic point defects, defects connected to H_2, O_2 or H_2O, and (inner) surfaces. Our calculations show that most subgap levels originating from stretched bonds, silane (SiH) or silanol (SiOH) groups concentrate in a range of 0–2 eV around the band edges. For an energy of ~3.5 eV, like that of lasers in the controlled fusion ignition at the National Ignition Facility (NIF), these subgap levels do not cause absorption of such photons due to the large band gap ≥8 eV of a-SiO_2. However, E'-centers (≡Si•), non bridging oxygen hole centers (NBOHC, ≡Si–O•) and peroxy linkages (POL, ≡Si–O–O–Si≡) may act as possible source of absorption. The addition of hydrogen can reduce the number of those defect levels in the middle of the band gap by shifting them to the band edges.

1. Introduction

On December 5, 2022 a controlled ignition of a nuclear fusion reaction with a positive energy balance was demonstrated for the first time at the National Ignition Facility (NIF) in the USA. This important milestone on the road to inertial confinement fusion generated 3.1 (±0.16) MJ of nuclear energy [1]. To drive the fusion reaction of a compressed fuel capsule, the NIF laser system (wavelength 351 nm), in conjunction with numerous optical components, delivered a highly precise pulse shape with 2.05 MJ laser energy. A key aspect of laser-driven inertial confinement fusion concerns the finite laser-induced damage threshold of optical materials. The exposure of silica glass to intensive radiation of high energy leads to the degradation of its optical properties. Therefore, large-aperture lenses are used to achieve a distribution of the laser pulse energy over large cross-sections, using substrates made of high-purity materials with a large band gap like silica glass (a-SiO_2) containing as few defects as possible.

There are numerous experimental and theoretical studies elucidating the creation and optical absorption of defects in a-SiO_2 [2–21]. The review of Salh [22] offers a detailed and clear overview of possible defect types and proposed level schemes. Further summaries of the main optical properties of point defects and impurities can be found in Skuja et al. [23] and Girard et al. [24].

The challenge of developing a comprehensive theoretical description is twofold. On the one hand, it is important to cover the variety of structural defects in a-SiO_2 and, on the other hand, to apply a suitable modeling approach that allows a good description of the generated defect levels for this wide band gap material. The density functional theory (DFT) study of Szymanski et al. [7] on the effects of interstitial oxygen demonstrated the importance of taking into account the disorder of a-SiO_2 and concluded that it is not sufficient to consider only single crystal models. Also Winkler et al. [9] showed how site-to-site disorder directly smears the electronic level structure using the example of peroxy linkages (POL, also called peroxy bridge, ≡Si–O–O–Si≡). From the analysis of eleven atomistic a-SiO_2 structure models they derived a broad absorption band of range 3.2–7.5 eV for POLs using the GW quasiparticle approximation invented by Hedin [25–28]. This method yields a good description of wide band gap oxides but is computationally demanding. Defect levels were also calculated by Donglin et al. [11] who used a computationally expensive hybrid exchange–correlation functional [29] for the simulation of non-bridging oxygen

* Corresponding author.
E-mail address: wolfgang.koerner@iwm.fraunhofer.de (W. Körner).

https://doi.org/10.1016/j.jnoncrysol.2026.124332
Received 22 May 2026; Received in revised form 29 July 2026; Accepted 24 August 2026
Available online 3 September 2026
0022-3093/© 2026 The Authors. Published by Elsevier B.V. This is an open access article under the CC BY license (http://creativecommons.org/licenses/by/4.0/).

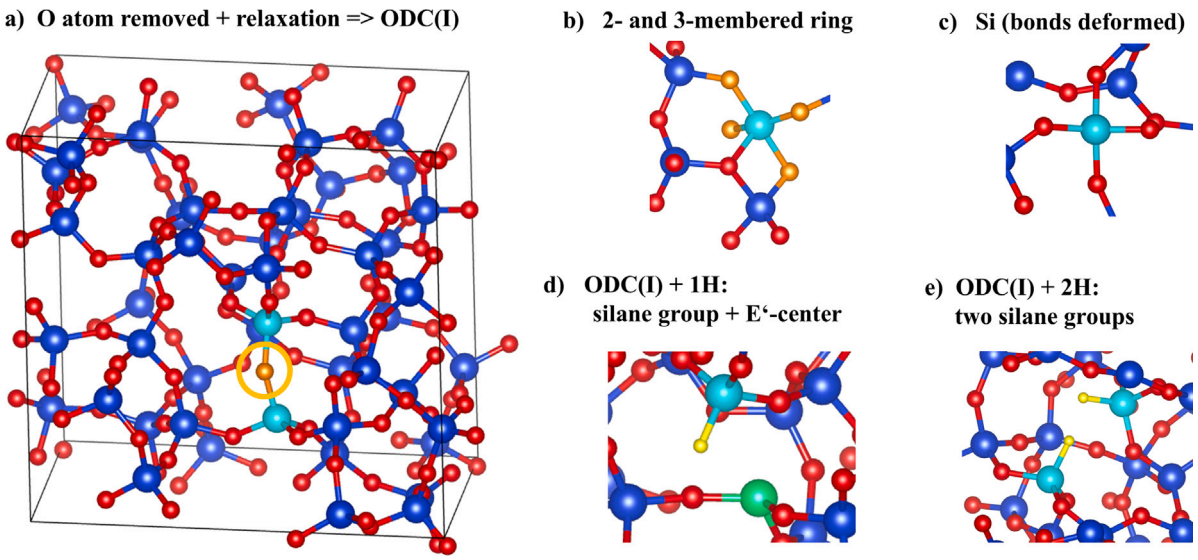

Fig. 1. (Color online) Atomistic models of a-SiO_2 containing point defects: (a) complete supercell of model 3 (removal of the encircled O atom and subsequent structural relaxation creates an ODC(I)) defect (≡Si–Si≡), (b) 2- and 3-membered ring in model 6 (the highlighted atoms in light blue (Si) and orange (O)) cause ~85% of the subgap states (dashed blue line in Fig. 3), (c) miscoordinated Si atom: the four Si–O bonds are almost in one plane and not in tetrahedral orientation, (d) ODC+1H: silane group (Si-H) and E′-center (≡Si•) and (e) ODC+2H: two silane groups. Si atoms are represented by big spheres in blue, green or light blue, where the latter two highlight Si atoms belonging to point defects. Oxygen atoms are shown by medium red spheres and hydrogen atoms by small yellow spheres.

defects and oxygen vacancy defects at the expense of studying only few defect realizations.

The main objective of our study is the analysis of defects in a-SiO_2 and to identify those that cause optical absorption bands for photon energies of about 3.5 eV, which corresponds to the wavelength of the NIF laser [1]. By means of atomistic DFT simulations, we investigate various kinds of deviations from the perfectly stoichiometric and relaxed a-SiO_2 network: strained bonds in small rings of size two or three, intrinsic point defects due to missing Si or O atoms, and additional H or O atoms. By creating 10 to 15 realizations for each of the considered non-stoichiometric defects we end up with 114 supercell models (with up to 327 atoms) for which we evaluated and analyzed the electronic density of states (DOS). Since the SiO_2 glass used in the NIF experiments is exposed to photons and other elementary particles of high intensities and high energies, the formation of voids or pores inside the glass is likely. In order to model voids that are large compared to interatomic bond lengths, we consider supercell models with flat surfaces that have unsaturated bonds, silane (SiH), silanol (SiOH), or mixed termination.

The paper is organized as follows. In Section 2 we introduce the details of our computational approach. In Section 3 we present the electronic DOS of the aforementioned structural defects and compare the results to experimental and other theoretical studies. Furthermore, we discuss the relevance of the defect levels concerning the optical absorption in the range of UV light and possible methods to remove these defect levels. A summary in Section 4 concludes the paper.

2. Theoretical approach

2.1. Structure models

Our study is based on ten stoichiometric atomistic structure models of a-SiO_2, each containing 50 Si and 100 O atoms, which we have taken from previous work [30]. The average density of our set of ten supercell models is 2.20 g/cm^3 [31]. The cells have an approximately cuboidal shape and an edge length of ~13 Å. Fig. 1(a) displays our model 3 as an example. The average supercell volume is 2274 Å^3 with a standard deviation of 63 Å^3. Thus our supercells sample regions of higher and lower density in a-SiO_2. Our average Si–O bond length of 1.639 Å is 1.9% longer than the 1.608 ± 0.04 Å determined experimentally by Grimley et al. [32]. For the O–Si–O bond angle, our 109.5° agree with the experimental value of 109.7° ±0.6° within the experimental uncertainty.

Five of our ten supercells contain a three-membered ring, meaning a ring that contains three Si atoms connected by three O atoms (n-membered rings are denoted as n-rings in the following). In one supercell there is a two-membered ring which is also called 2-Bridging Oxygen Center [33].

Starting from these ten supercell models of a-SiO_2 we have created intrinsic point defects by removing either individual Si or O atoms, and adding H atoms (15 models per case). Our approach thus creates pairs of Si dangling bonds (commonly denoted as E′-centers) when removing one O atom, and up to four non-bridging oxygen hole centers (commonly abbreviated by NBOHC) when removing one Si atom. By saturating all dangling bonds except one we can obtain individual E′-centers or NBOHC defects.

As final step, we performed structural relaxations in the framework of the DFT in order to optimize the atomic positions and cell parameters so that we minimize the total energy. We used the PWscf code of the Quantum Espresso software package [34,35] employing Standard Solid State Pseudopotentials (SSSP *Efficiency* version 1.3.0) [36,37] and the Perdew–Burke–Ernzerhof (PBE) [38] exchange–correlation functional. The wave functions of the valence electrons are represented by a plane-waves basis set with a cutoff energy of 50 Ry (1 Rydberg ≈ 13, 606 eV), and the electron density and effective Kohn–Sham potential by discrete Fourier series with a cutoff energy of 400 Ry. Given the size of the supercells, the Brillouin zone was sampled at the Gamma point only. The convergence threshold was set to 10^{-3} Ry for the total energy and to 10^{-3} Ry/Bohr (1 Bohr ≈ 0.529 Å) for the forces on atoms. Elastic stresses and atomic forces were relaxed using the Broyden–Fletcher–Goldfarb–Shanno (BFGS) algorithm.

For the calculation of point defects in crystalline α-quartz we have tripled the primitive unit cell in all three spatial directions. The obtained supercell contains 243 atoms with dimensions of ~15.0 × 13.0 × 16.5 Å^3.

For the determination of surface states we have doubled three of ten a-SiO_2 model structures with 150 atoms in one direction and added an empty supercell of the same size. The cells have approximately rectangular shapes of three stacked cuboids with dimensions of

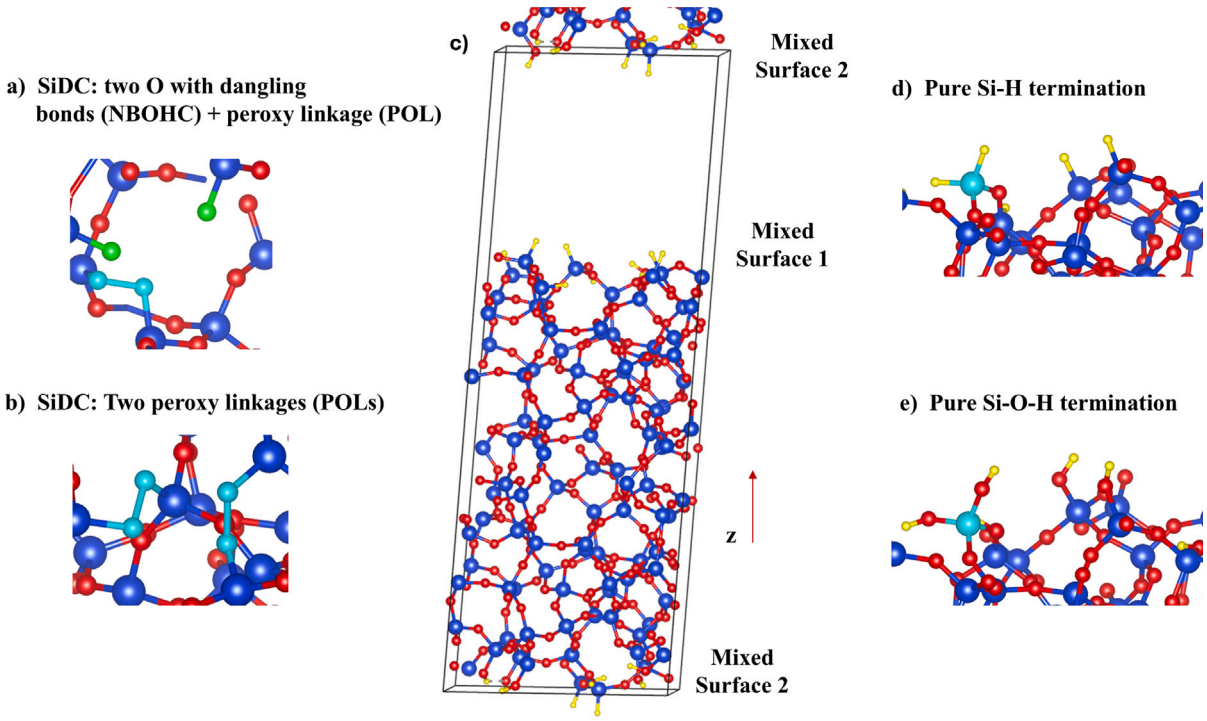

Fig. 2. (Color online) Atomistic models of (a) a silicon deficiency center (SiDC) which relaxed to two oxygen dangling bonds, also named non-bridging oxygen hole centers (NBOHCs, ≡Si–O•), and one peroxy linkage (POL), (b) SiDC which formed two POLs, (c) surface supercell model with mixed SiH and SiOH termination, (d) a-SiO_2 surface with SiH termination and (e) a-SiO_2 surface with SiOH termination. Si atoms are represented by big spheres in dark blue, oxygen atoms by medium spheres in red and hydrogen atoms are shown by small yellow spheres. Atoms belonging to defects are highlighted in green or light blue.

~13 × 13 × 39 Å^3. The ~13 Å thick layer of empty space ensures that the two surfaces in the supercells do not interact with each other. For the surface termination we have chosen pure SiH, pure SiOH and mixed SiH/SiOH terminations (see Fig. 2). Furthermore, we have built surface models with single Si dangling bonds or NBOHCs by removing one H atom from SiOH or SiH groups at the surface. The supercell models contain 300–327 atoms. In the case of pure SiOH termination, our surface density of OH groups varies in a range of 4.6–5.8 nm^{-2} which fits well to the 4.9 nm^{-2} determined in experiments [39].

Since we have numerous supercell models with 300 or more atoms, we have opted for a fast and efficient approach for the calculation of the electronic DOS, which will be explained in the following subsection.

2.2. Electronic density of states

The most widely used DFT approximations for the exchange–correlation potential are the local-density approximation (LDA) and the generalized gradient approximations (GGA). They describe many ground-state properties with good accuracy and reliability. However, in the case of wide band gap semiconductors the calculated electronic band gaps are significantly smaller than those from experiments (see e.g. Refs. [40–42]). The reason for these discrepancies are due to the lack of a discontinuity of the exchange–correlation potential for the single-particle excitation of an electron going from the valence band to the conduction band. Most methods developed for overcoming these limitations like, e.g., the GW quasiparticle approximation [25–28], hybrid functionals [43], or screened exchange LDA (SX-LDA) [44] increase the computational costs significantly. Therefore, we have opted for the DFT-1/2 approach developed by Ferreira and coworkers [45]. Like the self-interaction-correction (SIC) [40,42,46], the DFT-1/2 self-energy correction is incorporated in the pseudopotentials and thus requires no additional computational effort compared to LDA or GGA calculations.

For the determination of the electronic DOS we use the Vienna Ab Initio Simulation Package (VASP) [47,48]. Mao et al. [49] provide a pseudopotential generation tool that creates DFT-1/2 corrected potentials compatible to the DFT potentials of VASP. We used α-quartz SiO_2 (space group $P3_221$) for the adjustment procedure of the potentials of Si and O, which resulted in optimized cutoff radii CUT = 4.9 Bohr for silicon and CUT = 2.5 Bohr for oxygen, when using an exponent n = 8 (see Ref. [45] for details on the adjustment procedure).

For all VASP calculations the Bloch waves of the valence electrons are expanded in a plane-waves basis with a cutoff energy of 520 eV and the interactions of the valence electrons and the ionic cores are included by projector-augmented-waves (PAW) potentials [50]. The exchange–correlation energy and potential are treated in GGA-PBE [38]. For the k-point sampling of the Brillouin-zone integrals a Monkhorst–Pack mesh of 3 × 3 × 3 points was used. For the surface models the equivalent k-point density was obtained with a mesh of 3 × 3 × 1. The Gaussian broadening was set to 0.1 eV. In the case of unpaired defect spins of E′-centers, NBOHCs and O_2 molecules spin-polarized calculations were done.

3. Results and discussion

For the following analysis of the electronic DOS we set the valence band (VB) edge of α-quartz to 0 eV. All other results are aligned by the oxygen 2s levels, which lie deeply below the band gap at about −20 eV to −17 eV. Since we discuss our results with respect to the possible absorption of UV light with photon energy of 3.5 eV, we have added arrows indicating selected possible transitions to some of the DOS plots for illustration.

3.1. Electronic DOS of defect free structures

The experimental band gap of α-quartz is 9.65 eV [51]. With our DFT-1/2-corrected pseudopotentials we obtained 9.05 eV. This value corresponds to the energy difference between the highest occupied energy level of the valence band and the lowest unoccupied energy

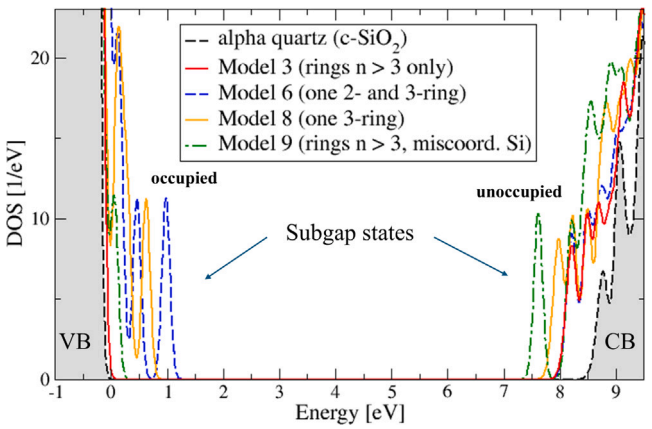

Fig. 3. (Color online) Electronic DOS of α-quartz and four a-SiO_2 models partially containing small n-rings ($n \leq 3$). The VB edge of α-quartz is set to 0 eV. Model 9 contains a miscoordinated Si atom (sketched in Fig. 1c).

level of the conduction band. In the subsequent figures, the energy ranges of the valence and conduction bands in the DOS graphs are shaded in gray. Note, however, that the unshaded region of the band gap between the two band edges is slightly smaller than the 9.05 eV due to the Gaussian smearing of 0.1 eV of all energy levels.

Although we still underestimate the band gap by 0.6 eV, the DFT-1/2 value is a considerable improvement compared to pure LDA (band gap 5.32 eV [52]) or our GGA-PBE value of 6.52 eV.

Fig. 3 compares the electronic DOS of four of our perfectly coordinated a-SiO_2 supercell models to the one of α-quartz. In all of these models, every Si atom has a fourfold coordination of O atoms, every O atom has a twofold coordination of Si atoms, and there is no additional H, O or H_2O present. However, such amorphous structure may contain 2-rings and 3-rings, which are sometimes also called defects (see e.g. Ref. [33]), although all their atoms are perfectly coordinated. Our model 8 contains one 3-ring and our model 6 has one 2-ring and one 3-ring, which are direct neighbors (see Fig. 1b).

Model 3 without any rings of size 2 or 3 shows the least smearing of the band edges compared to single crystal α-quartz. Models 6 and 8 have subgap states that reach up to ~1 eV in the band gap. An analysis of the site-projected DOS shows that the atoms in such small rings and their next-nearest neighbor atoms have shifted energy levels due to the locally strained atomic arrangement. Model 9 does not have small rings but contains one Si atom with extremely deformed coordination Here, all four Si-O bonds almost lie in one plane (see Fig. 1c), which causes the subgap state at ~7.6 eV. Thus not only small rings but also locally extreme arrangements for individual atoms can cause subgap states.

The smallest rings in model 3 are 4-rings. In the DOS they have the least deep levels. The main difference compared to the DOS of α-quartz is the broadening of the conduction band (CB) tail by ~0.5 eV. The band gaps of our defect-free a-SiO_2 supercell models are ~8.2 eV. A theoretical work of Winkler et al. using GW [9] yields 9.4 eV for defect-free a-SiO_2. These values are in the range of reported experimental values of 8.8 eV [53], 9.3 eV [54], and 11.5 eV [55]. The wide range of experimental values can be explained by different definitions and complications like the formation of excitons, presence of defects, and temperature-dependent Urbach tails (see e.g. Garvie et al. [56]).

Altogether, we conclude that defect levels introduced by strained bonds of perfectly coordinated Si or O atoms are negligible for the absorption of UV light of energy 3.5 eV since the band gap between occupied and empty states is at least 6.5 eV.

3.2. Electronic DOS of oxygen deficient point defects

We have taken the two defect-free structure models 3 and 7 as starting cases for the construction of the following point defects. By the removal of one oxygen atom and subsequent structural relaxation we created 15 oxygen deficiency centers, named ODC(I) (see Fig. 1a). The ODC(I) defects give rise to an occupied defect band in the energy range 0.7–1.3 eV above the VB. The defect level of the corresponding oxygen vacancy in α-quartz lies at 1.1 eV (see green curve in Fig. 5) well within the energy range of the amorphous defect band.

Furthermore, ODC(I) defects cause empty states down to ~1.2 eV below the CB edge (see green curve in Fig. 4), mainly localized at the two undercoordinated Si atoms (Si–Si distance in a-SiO_2 is 2.443 (± 0.101) Å, and in α-quartz 2.446 Å). The respective unoccupied defect levels of oxygen vacancies in α-quartz do not lie in the band gap but at the CB edge (see green curve in Fig. 5).

By the addition of two H atoms to an ODC(I) defect, two silane groups are formed (see Fig. 1e). The empty states of the ODC(I) defects in a-SiO_2 can thereby be removed and occupied levels up to 2.5 eV appear above the VB (see ODC(I) + 2H, dashed orange curve in Fig. 4). For the oxygen vacancy in α-quartz, two occupied levels at 0.7 and 2.6 eV appear (see Fig. 5).

The addition of only one H atom to the ODC(I) defect yields one Si atom with only three oxygen neighbors (i.e. an E′-center) and one silanol group (depicted in Fig. 1d) after subsequent relaxation. Our set of E′-centers caused occupied levels in the range of 3.9–5.4 eV and unoccupied levels in the range of 6.2–7.4 eV. The occupied defect states localized at the E′-centers are relevant for the absorption of UV light since they are separated from the unoccupied levels at the bottom of the CB by around 3.5 eV (see red curve in Fig. 4).

By the addition of a H atom to an E′-center a silane group is formed and thus the absorption of light with 3.5 eV photon energy is no longer possible. Experimentally, oxygen vacancies were observed by Kajihara et al. [21] in crystalline and glassy SiO_2 with nearly similar optical absorption bands at 7.6 eV. Also earlier experimental work of Imai et al. [18] and Hosono et al. [19] on as-grown a-SiO_2 films ascribed an absorption band at 7.6 eV to the neutral ODC(I). Our calculated unoccupied levels for ODC(I) defects and E′-centers are thus consistent with their assignment when taking into account the ~0.6 eV too low CB edge of our approach.

According to the theoretical work of Robertson [3] silane groups produce a filled s-state just below the VB and an empty σ^*-state in the gap just below the CB. Experimentally, Skuja et al. [20] reported a small probability of photolysis of silane groups using a F_2 laser with an energy of 7.9 eV. Our range of occupied levels from 0 to 2.5 eV above the VB for silane groups makes an absorption of 7.9 eV UV light conceivable.

3.3. Electronic DOS of silicon deficient point defects

We created 15 silicon deficient centers (abbreviated SiDC in the following, in analogy to ODC) by the removal of one silicon atom from our defect-free a-SiO_2 structure models and subsequent relaxation. In about half of the cases we obtained two oxygen atoms with dangling bonds (≡Si–O•) and one peroxy linkage (≡Si–O–O–Si≡). An example of such a structure is shown in Fig. 2(a). In Fig. 6 the DOS of a typical case is depicted, in which two oxygen atoms with dangling bonds cause unoccupied defect levels at ~1.6 eV above the VB (red curve). The range of the defect levels connected to our NBOHCs is given in Table 1.

According to experiments [14–16], an oxygen dangling bond is a paramagnetic defect that may give a significant contribution to radiation-induced optical absorption in high purity silica in the visible and UV light. There are three major optical absorptions bands at 1.97, 4.8 and 6.8 eV (see e.g. Table 1 in Ref. [14]) assigned to NBOHC defects. Hosono et al. reported an intense optical absorption band centered at 6.8 eV with a fullwidth at half maximum (FWHM) of 1.76 eV. This broad optical absorption may be connected to excitations of electrons from the occupied defect levels we found in the range from 0 to 1.6 eV to the CB edge. The observed weak absorption at 1.97 eV

Table 1
Comparison of defect levels in the band gap of a-SiO_2 and α-quartz. Energies are given in eV relative to the VB of defect-free a-SiO_2 and α-quartz.

a-SiO_2	Occupied	Unoccupied	α-quartz	Occupied	Unoccupied
ODC(I) (≡Si–Si≡)	0.7–1.3	7.0–CB	O vacancy	1.1	at CB edge
E'-center (≡Si•)	3.9–5.4	6.2–7.4	E′-center	5.9	7.4
SiDC: NBOHC (≡Si–O•)	0.0–1.6	0.4–2.1	NBOHC	0.0–1.0	1.0–1.2
SiDC: POL (≡Si–O–O–Si≡)	0.2–2.2	4.5–6.5	Si vacancy (2 POL)	1.0, 1.3, 1.7	5.2
Silane group (≡Si–H)	0.0–2.5[a]	at CB edge	Silane group	0.7, 2.6	at CB edge
Silanol group (≡Si–O–H)	0.4[b]–2.0	7.8 to CB	Silanol group	0.6, 1.3	8.0 to CB

[a] For surface models silane levels up to ~3 eV were found.
[b] For surface models silanol levels down to ~0 eV were found (see Section 3.5).

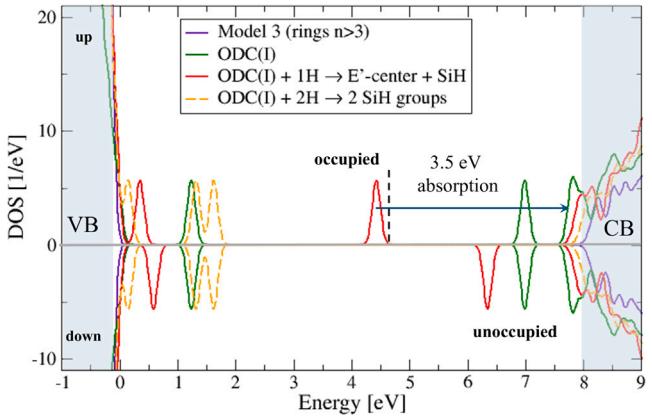

Fig. 4. (Color online) Electronic DOS of defect-free a-SiO_2 (Model 3) compared to that of an ODC(I) defect with different amounts of hydrogen, generated from this structure model. The ODC(I) defects cause occupied defect up to 1.2 eV above the VB and empty states down to –1 eV below the CB. Adding one H atom creates a silane group (occupied levels above the VB) and a E′-center with defect levels in the upper half. Adding two H atoms to an ODC(I) leads to levels above the VB which are localized at the two formed Si-H groups.

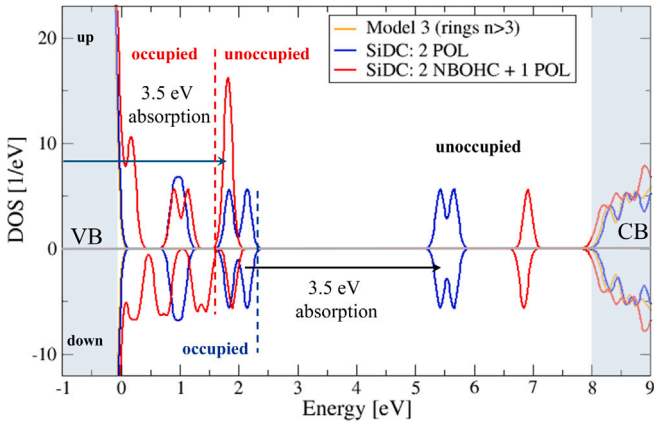

Fig. 6. (Color online) Spin-resolved electronic DOS of defect-free a-SiO_2 (Model 3) and two typical SiDC models in a-SiO_2. SiDC defects can cause unoccupied defect levels (NBOHC) which are relevant for UV absorption (here at ~1.6 eV, see vertical red dashed line). The addition of hydrogen reduces the number of NBOHC defects forming lower lying silanol groups. If a SiDC turns into two POLs there are no unoccupied levels above the VB but electrons can be lifted to the unoccupied levels in the upper half of the band gap (blue curve).

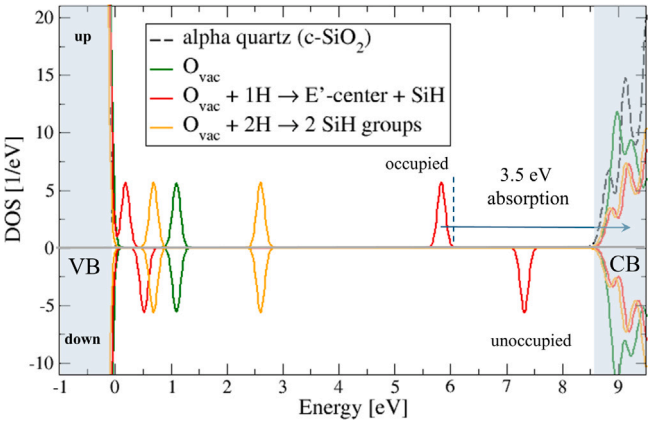

Fig. 5. (Color online) Electronic DOS of defect-free α-quartz and an oxygen vacancy (O_{vac}) with different amounts of hydrogen. The oxygen vacancy in α-quartz causes a defect level 1.1 eV above the VB. Adding one H atom creates a silane group (occupied levels above the VB) and a E′-center with defect levels in the upper half, which can cause absorption of UV light of 3.5 eV energy. Adding two H atoms leads to Si–H groups with levels ~2.5 eV above the VB and thus avoids absorption.

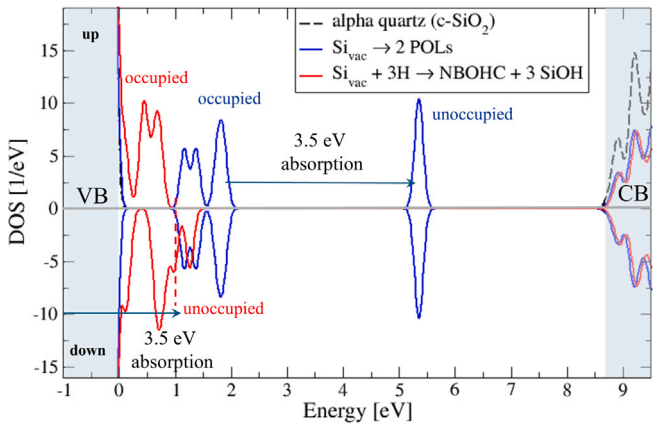

Fig. 7. (Color online) Electronic DOS of defect-free α-quartz, a silicon vacancy (Si_{vac}) recombined to two POL, and with 3 H atoms added, which corresponds to one NBOHC and three silanol groups. Like in the case of a-SiO_2, POL and NBOHC defects can cause absorption of UV light of 3.5 eV energy.

(FWHM of 0.17 eV) [15] may be connected to excitation from the VB to our unoccupied levels in the range from 0.4 eV to 2.1 eV above the VB. In α-quartz we find the unoccupied NBOHC levels between 1.0 and 1.2 eV (see red curve in Fig. 7).

For the strong absorption band at 4.8 eV (FWHM of 1.07 eV) we do not find an excitation paths in our results. This might be due to the fact that our models do not represent all possible realizations of NBOHC defects. For instance, NBOHCs in isolated form cannot be modeled well within the rather small size of the supercell models limited by the computational resources for the DFT calculations.

Seven of the 15 relaxed SiDC defects resulted in pairs of peroxy linkages (c.f. Fig. 2b). This defect complex does not have low lying unoccupied states above the VB edge (c.f. blue curve in Fig. 6). However, the energy difference between the occupied gap states and the unoccupied gap states is less than 3.5 eV, and thus also peroxy bridges may cause UV absorption. The variety of energy ranges of the defect levels is given in Table 1.

The removal of a silicon atom in α-quartz and subsequent relaxation (silicon vacancy in α-quartz) has lead to two POLs which cause three occupied defect levels at 1.0, 1.3 and 1.7 eV, and an unoccupied level at 5.2 eV, lying within the bands obtained for the POLs in a-SiO_2 (see Fig. 7).

Calculations of O'Reilly and Robertson [2] already suggested that peroxy linkages are the lowest energy configuration for interstitial oxygen in a-SiO_2. There are numerous theoretical results for the optical absorption bands of POLs: 4.4(0.1) eV [6], 5.5 eV [5], 6.5(0.3) eV [4], and 8.6 eV [2]. Our results coincide mostly with the recent work of Winkler et al. (absorption band ranging from 3.2 to 7.5 eV) [9]. Excitations from the occupied defect levels above the VB edge to empty levels between 4.5 to 6.5 eV are possible with at least 3.3 eV, and excitations directly into the CB require up to about 7 eV.

The addition of hydrogen can saturate the dangling oxygen bonds, and silanol groups are formed. For our a-SiO_2 models we found occupied defect levels in the range 0–2 eV above the VB edge. Excitations from the occupied levels to the CB require at least 7 eV energy.

Experimentally, Vella et al. [13] attributed a peak between ~7.5 eV and ~8.1 eV to the absorption of the Si–OH group, which fits well to the occupied levels between 0.4 eV and 2 eV above the VB found in our calculations, because energies of 7 to 8 eV are needed to excite electrons from these low lying states to the lower tail of the CB of a-SiO_2. Thus hydrogen doping can reduce the UV absorption in this case. That is why hydrogen loading is efficient for radiation hardening [57] (see also Ref. [24] and references therein).

Note that with our present study of the electronic structure of statically relaxed configurations of defect complexes in amorphous structures we cannot answer the question to what extent hydrogen can break peroxy bridges and what temperatures are necessary for this process. This may be the topic of a future study on the kinetics of the formation or healing of defect complexes in a-SiO_2.

3.4. Electronic DOS of interstitial molecules in a-SiO_2 voids

Apart from the defects discussed in the previous subsections, also small interstitial molecules may be present in the amorphous network and influence the electronic structure. Experiments have shown an increase in the intensity of the absorption bands of molecules compared to the gas phase [58,59] which is explained by the confinement of the excited-state wave functions by the SiO_2 network, which causes an increased overlap with the ground-state wave function [60].

We have put H_2, O_2 and H_2O molecules in small (diameter ≤6 Å), medium (diameter ~8 Å) and large voids (diameter ≥10 Å) inside amorphous silica networks, either close to the centers or close to the surface of these voids. In all considered cases, O_2 and H_2 never bind to the a-SiO_2 network. The energy of the defect levels of O_2 molecules increase with the size of the void (compare red and green curves in Fig. 8).

The peaks below the dashed lines in Fig. 8 refer to energy levels filled with single electrons for the blue, green and yellow curves and to degenerate energy levels filled with two electrons for the red curve. Therefore, for O_2 molecules inside SiO_2 voids the highest two one-electron states are either spin up (red curve) or spin down (green curve) forming together the electron-pair triplet state. The level splitting in smaller voids can be explained by the non-spherical shape of the voids. The resulting reduced energy distance of occupied and unoccupied levels may contribute to the observed redshift of the optical UV absorption observed in experiments [58].

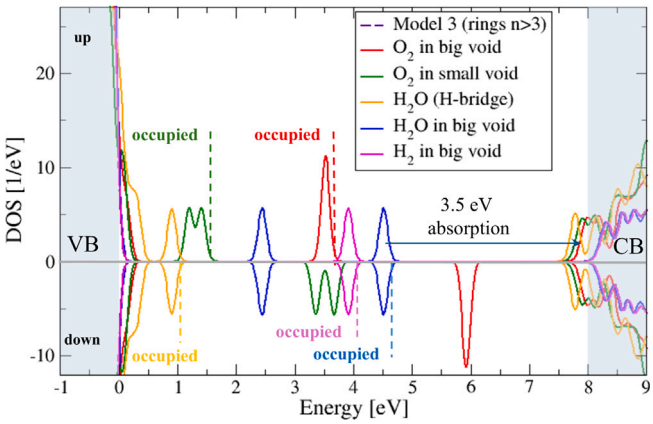

Fig. 8. (Color online) Spin-resolved electronic DOS of defect-free a-SiO_2 (Model 3), H_2O attached by H-bridges to the a-SiO_2 network or unattached. O_2 molecules do not bind to the a-SiO_2 network. In small voids their subgap levels are lower than in big voids.

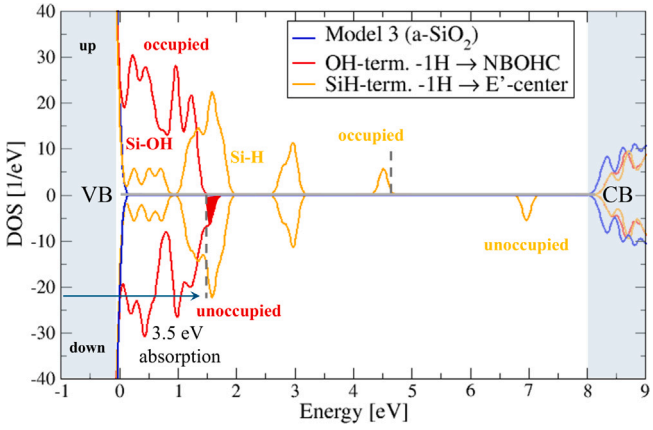

Fig. 9. (Color online) Electronic DOS of bulk a-SiO_2 (Model 3), an amorphous sample containing two surfaces with OH termination, where at one position the H atom is removed which leads to an E′-center, and a surface model with SiH termination, where one missing H leads to a NBOHC. Like in bulk a-SiO_2 the silanol groups at the surface cause subgap states up to 2 eV above the VB. For the silane groups deeper levels up to about 3 eV above the VB were found. The NBOHC causes empty states at about 1.5 eV above the VB (highlighted in red) which may cause absorption. The occupied states of E′-center are located in the middle of the band gap.

By relaxation, some of the H_2O molecules got attached by H-bridges to the a-SiO_2 network. They give rise to low lying levels above the VB edge. This is qualitatively consistent experiments where the UV absorption band of interstitial H_2O is blue-shifted compared to H_2O in gas phase [58]. Unbound H_2O molecules result in higher levels for which absorption of 3.5 eV energy may be possible (see blue curve in Fig. 8) in case that there is a sufficient overlap of wave functions of the initial and final states.

3.5. Electronic DOS of surfaces states

This section is dedicated to surface states at flat outer surfaces which may appear also at inner surfaces of large voids that can be created by intensive application of energy. Note that our surface model systems do not take into account stress fields and chemical potential fields introduced during polishing or contamination with other elements.

In the previous sections we discussed defect levels connected to H and OH in bulk a-SiO_2 and showed that the addition of hydrogen

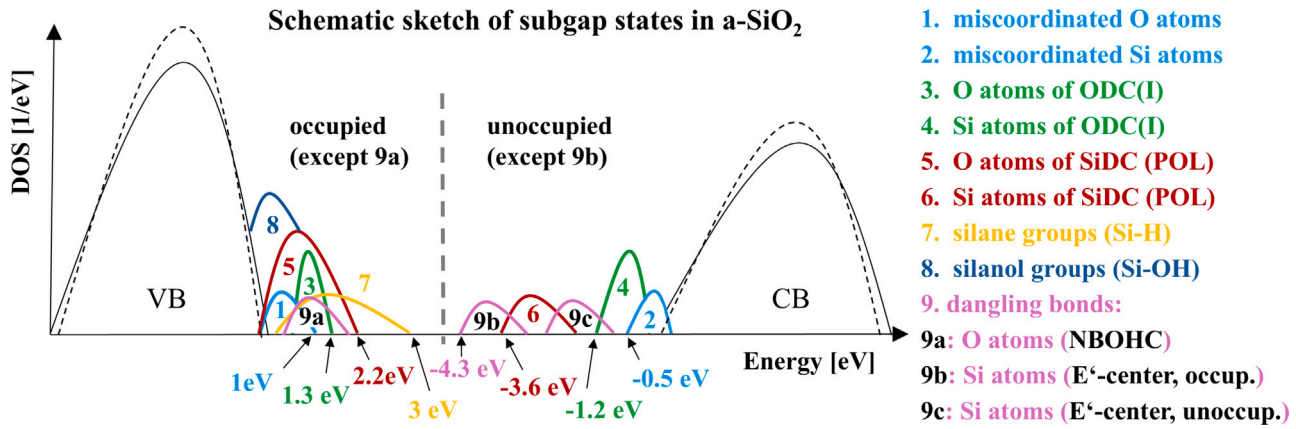

Fig. 10. (Color online) Schematic summary of the electronic DOS of α-quartz (black dashed line), defect-free a-SiO_2 (black solid line) and various defect bands. Energy values are given relative to VB and CB of defect-free a-SiO_2. Levels in the lower half of the band gap are mostly occupied. The only exceptions are levels of silicon or oxygen atoms with dangling bonds (e.g. part of SiDC).

moves subgap levels caused by dangling bonds to the band edges. This situation is similar for surfaces with silane or silanol termination, as can be seen in Fig. 9. The positions of defect levels due to silanol groups at the surface are similar to the those in bulk a-SiO_2 distributed from 0 to about 2 eV above the VB edge. We obtained defect levels up to about 3 eV for the silane groups at surfaces which is 0.5 eV higher than for bulk a-SiO_2. A structural analysis revealed that the levels higher than 2.5 eV originate from surface Si atoms which are saturated with two H atoms (see Fig. 2d). Similarly, two OH groups bound to the same Si (shown in Fig. 2e) cause higher levels up to 2 eV than single OH groups. However, for defects like SiDC + 4H in bulk a-SiO_2, forming four silanol groups, we have also found levels up to 2 eV.

For mixed silane/silanol termination (not shown) the distribution of subgap levels is a combination of rather shallow lying silanol levels and rather deep lying silane levels in the range 0–3 eV.

Individual E′-centers and NBOHCs at the surface of our models caused occupied and unoccupied levels that lie in the same energy ranges as in the bulk models.

If the highest occupied level of an E′-center is high enough (c.f. red curve in Fig. 4), absorption of 3.5 eV light is possible. In the case of the E′-center shown in Fig. 9 (orange curve), the energies of the highest occupied levels are too low. Thus, according to our calculations, E′-centers in bulk a-SiO_2 are possible with energy levels, that allow absorption of light of 3.5 eV photon energy. However, we cannot quantify whether the concentration of such E′-centers could be high enough for leading to a significant feature in an absorption spectrum.

In contrast, according to our calculations, NBOHC with their low lying unoccupied states may always absorb photons of 3.5 eV (see e.g. red curve in Fig. 9), which is an experimentally established fact (see e.g. Skuja et al. [16]).

Dangling bonds at outer or inner surfaces need to be avoided for a good transparency of silica glass because otherwise multiple absorption processes arise. The occupied silanol/silane defect levels are unproblematic as long as empty defect states nearby lie higher than ~7 eV.

4. Summary and conclusions

We have constructed a set of atomistic structure models of a-SiO_2 containing various defects: single atoms in a distorted neighborhood (like e.g. the miscoordinated Si atom shown in Fig. 1c), 2- and 3-rings, oxygen and silicon deficiencies without or with varying numbers of attached H atoms, surfaces with SiH, SiOH or mixed termination, and dangling bonds at Si or O atoms. For all these defects we have evaluated the electronic DOS by DFT-1/2 calculations. For comparison, we have constructed atomistic models of α-quartz containing the corresponding Si and O vacancies plus different numbers of attached H atoms. In summary, the defect levels in a-SiO_2 always lie in the same energy range as the respective defect levels of the α-quartz.

We summarize the obtained variety of defect bands in a schematic sketch in Fig. 10. Shallow defect levels at the VB and CB edges stem from Si and O atoms which are fourfold or twofold coordinated, respectively, but the lengths and angles of their bonds to the next neighbors deviate significantly from the single crystal values (see bands marked as 1 and 2 in Fig. 10). The defect levels due to local oxygen deficiencies (ODC(I)) spread ~1.3 eV above the VB and ~ − 1.2 eV below the CB (bands 3 and 4 in Fig. 10). The addition of H atoms to ODC(I) defects saturates the dangling bonds at Si atoms and silane groups are formed (band 7). In bulk a-SiO_2, levels of silane groups appeared up to ~2.2 eV. For our surface models, levels of silane groups were found up to ~3 eV.

Local Si deficiencies relaxed to two POLs causing occupied defects levels up to ~2.2 eV above the VB edge (band 5) and deep lying empty levels (band 6). These bands are relevant for absorption of laser light with a photon energy of 3.5 eV. Relevant absorption bands were created in the case when silicon deficiency centers did not form POLs but NBOHCs (dangling O atoms). In Fig. 10 the unoccupied levels which can be filled by electrons from the VB range from 0.4–2.1 eV (band 9a). The addition of hydrogen to SiDCs creates silanol groups. As a result, all empty states are removed and a defect band up to ~2 eV above the VB edge remains (band 8).

Threefold coordinated Si atoms (E′-centers) lead to occupied defect states in the range of 3.9–5.4 eV (band 9b) and unoccupied defect states in the range of 6.2–7.4 eV (band 9c). The former levels can cause absorption of ~3.5 eV photons. By the addition of H atoms, silane groups are formed which closes this absorption channel since occupied levels below 2.5 eV are formed.

However, only partial saturation of ODC(I) and SiDC with hydrogen creates E′-centers and NBOHC which cause absorption of light with energy 3.5 eV.

Intercalated H_2, O_2 and H_2O molecules lead to occupied levels in the lower half of the band gap and unoccupied levels. For H_2O molecules we expect a possibility of weak absorption of photons with energy 3.5 eV.

CRediT authorship contribution statement

Wolfgang Körner: Writing – original draft, Investigation, Data curation, Conceptualization. **Manuel Enns:** Writing – review & editing, Methodology, Data curation. **Peter Gumbsch:** Writing – review & editing, Funding acquisition. **Daniel F. Urban:** Writing – review & editing, Methodology. **Christian Elsässer:** Writing – review & editing, Supervision, Funding acquisition, Conceptualization.

Declaration of competing interest

The authors declare that they have no known competing financial interests or personal relationships that could have appeared to influence the work reported in this paper.

Acknowledgments

Funding for this work was provided by the German Federal Ministry of Research, Technology and Space (BMFTR) within the framework of the collaboration research project "Anti-reflective metasurfaces on materials with large band gaps (nanoAR, support number 13F1007G)".

References

[1] H. Abu-Shawareb, et al., Phys. Rev. Lett. 132 (2024) 065102, http://dx.doi.org/10.1103/PhysRevLett.132.065102.
[2] E.P. O'Reilly, J. Robertson, Theory of defects in vitreous silicon dioxide, Phys. Rev. B 27 (1983) 3780, http://dx.doi.org/10.1103/PhysRevB.27.3780.
[3] J. Robertson, in: Roderich A.B. Devine (Ed.), The Physics and Technology of Amorphous SiO_2, National center for Telecommunication Studies, Meyland, France, 1988.
[4] G. Pacchioni, G. Ierano, Ab initio theory of optical transitions of point defects in SiO2, Phys. Rev. B 57 (1998) 818, http://dx.doi.org/10.1103/PhysRevB.57.818.
[5] B.B. Stefanov, K. Raghavachari, Photoabsorption of the peroxide linkage defect in silicate glasses, J. Chem. Phys. 111 (1999) 8039, http://dx.doi.org/10.1063/1.480137.
[6] D. Ricci, G. Pacchioni, M.A. Szymanski, A.L. Shluger, A.M. Stoneham, Modeling disorder in amorphous silica with embedded clusters: The peroxy bridge defect center, Phys. Rev. B 64 (2001) 224104, http://dx.doi.org/10.1103/PhysRevB.64.224104.
[7] M.A. Szymanski, A.L. Shluger, A.M. Stoneham, Role of disorder in incorporation energies of oxygen atoms in amorphous silica, Phys. Rev. B 63 (2015) 224207, http://dx.doi.org/10.1103/PhysRevB.63.224207.
[8] Y. Cheng, D. Ren, H. Zhang, X. Cheng, First-principle study of the structural, electronic and optical properties of defected amorphous silica, J. Non-Cryst. Solids 416 (2015) 36, http://dx.doi.org/10.1016/j.jnoncrysol.2015.02.006.
[9] B. Winkler, L. Martin-Samos, N. Richard, L. Giacomazzi, A. Alessi, S. Girard, A. Boukenter, Y. Ouerdane, M. Valant, Correlations between structural and optical properties of peroxy bridges from first principles, J. Phys. Chem. C 121 (7) (2017) 4002, http://dx.doi.org/10.1021/acs.jpcc.6b11291.
[10] L. Li, X. Chen, H. Zhou, et al., First principle studies on properties of Silicon-vacancy related defects in amorphous silica, J. Non-Cryst. Solids 594 (2022) 121799, http://dx.doi.org/10.1016/j.jnoncrysol.2022.121799.
[11] C. Donglin, D. Shangli, L. Hai, Z. Xudong, First principles calculations of electronic structure and optical properties for radiation-induced oxygen related defects in silica glass, J. Non-Cryst. Solids 666 (2025) 123665, http://dx.doi.org/10.1016/j.jnoncrysol.2025.123665.
[12] H. Nishikawa, R. Tohmon, Y. Ohki, K. Nagasawa, Q. Hama, Defects and optical absorption bands induced by surplus oxygen in highpurity synthetic silica, J. Appl. Phys. 65 (1989) 4672, http://dx.doi.org/10.1063/1.343242.
[13] E. Vella, R. Boscaino, G. Navarra, Vacuum-ultraviolet absorption of amorphous SiO_2: Intrinsic contribution and role of silanol groups, Phys. Rev. B 77 (2008) 165203, http://dx.doi.org/10.1103/PhysRevB.77.165203.
[14] H. Hosono, K. Kajihara, T. Suzuki, Y. Ikuta, L. Skuja, M. Hirano, Vacuum ultraviolet optical absorption band of non-bridging oxygen hole centers in SiO2 glass, Solid State Commun. 122 (2002) 117, http://dx.doi.org/10.1016/S0038-1098(02)00118-7.
[15] L. Skuja, G. Pacchioni, L. Skuja, D.L. Griscom (Eds.), Defects in SiO2 and Related Dielectrics: Science and Technology, Kluwer Academic Publishers, Dordrecht, 2001, pp. 73–116.
[16] L. Skuja, K. Kajihara, M. Hirano, H. Hosono, Visible to vacuum-UV range optical absorption of oxygen dangling bonds in amorphous SiO 2, Phys. Rev. B 84 (20) (2011) 205206, http://dx.doi.org/10.1103/PhysRevB.84.205206.
[17] S. Girard, J. Kuhnhenn, A. Gusarov, B. Brichard, M. Van Uffelen, Y. Ouerdane, et al., Radiation effects on silica-based optical fibers: Recent advances and future challenges, IEEE Trans. Nucl. Sci. 60 (3) (2013) http://dx.doi.org/10.1109/TNS.2012.2235464.
[18] H. Imai, K. Arai, H. Imagawa, H. Hosono, Y. Abe, Two types of oxygen-deficient centers in synthetic silica glass, Phys. Rev. B 38 (1988) 12772, http://dx.doi.org/10.1103/PhysRevB.38.12772.
[19] H. Hosono, Y. Abe, H. Imagawa, H. Imai, K. Arai, Experimental evidence for the Si-Si bond model of the 7.6-eV band in SiO2 glass, Phys. Rev. B 44 (1991) 12043, http://dx.doi.org/10.1103/PhysRevB.44.12043.
[20] L. Skuja, K. Kajihara, M. Hirano, H. Hosono, Fluorine laser-induced silicon hydride Si–H groups in silica, J. Non-Cryst. Solids 353 (2007) 526, http://dx.doi.org/10.1016/j.jnoncrysol.2006.10.020.
[21] K. Kajihara, L. Skuja, H. Hosono, Formation and annihilation of intrinsic defects induced by electronic excitation in high-purity crystalline SiO2, J. Appl. Phys. 113 (14) (2013) http://dx.doi.org/10.1063/1.4800961.
[22] R. Salh, Defect related luminescence in silicon dioxide network: a review, in: B. Sukumar (Ed.), Crystalline Silicon - Properties and Uses, InTech, Rijeka, 2011, pp. 135–172.
[23] L. Skuja, M. Hirano, H. Hosono, K. Kajihara, Defects in oxide glasses, Phys. Status Solidi (C) c (1) (2005) 15–24, http://dx.doi.org/10.1002/pssc.200460102.
[24] S. Girard, et al., Overview of radiation induced point defects in silica-based optical fibers Overview of radiation induced point defects in silica-based optical fibers, Rev. Phys. 4 (2019) 100032, http://dx.doi.org/10.1016/j.revip.2019.100032.
[25] L. Hedin, New method for calculating the one-particle Green's function with application to the electron-gas problem, Phys. Rev. 139 (3A) (1965) A796–A823, http://dx.doi.org/10.1103/PhysRev.139.A796.
[26] M.S. Hybertsen, S.G. Louie, First-principles theory of quasiparticles: Calculation of band gaps in semiconductors and insulators, Phys. Rev. Lett. 55 (1985) 1418, http://dx.doi.org/10.1103/PhysRevLett.55.1418.
[27] M. van Schilfgaarde, T. Kotani, S.V. Faleev, Quasiparticle self-consistent GW theory, Phys. Rev. Lett. 96 (2006) 226402, http://dx.doi.org/10.1103/PhysRevLett.96.226402.
[28] M. van Schilfgaarde, T. Kotani, S.V. Faleev, Adequacy of approximations in GW theory, Phys. Rev. B 74 (2006) 245125, http://dx.doi.org/10.1103/PhysRevB.74.245125.
[29] M. Guidon, J. Hutter, J. VandeVondele, Robust periodic hartree-fock exchange for large-scale simulations using Gaussian basis sets, J. Chem. Theory Comput. 5 (2009) 3010, http://dx.doi.org/10.1021/ct900494g.
[30] M. Enns, W. Körner, C. Elsässer, D.F. Urban, Volume increase of silica glass due to water intercalation and silanol group formation, J. Non-Cryst. Solids 674 (2026) 123924, http://dx.doi.org/10.1016/j.jnoncrysol.2025.123924.
[31] S.R. Elliott, Physics of Amorphous Materials, second ed., Longman, Essex, 1990, p. 100.
[32] D.I. Grimley, A.C. Wright, R.N. Sinclair, Neutron scattering from vitreous silica IV. Time-of-flight diffraction, J. Non-Cryst. Solids 119 (1990) 49, http://dx.doi.org/10.1016/0022-3093(90)90240-M.
[33] A.V. Sulimov, D.C. Kutov, F.V. Grigoriev, A.V. Tikhonravov, V.B. Sulimov, Generation of amorphous silicon dioxide structures via melting-quenching density functional modeling, Lobachevskii J. Math. 41 (2020) 1581, http://dx.doi.org/10.1134/S1995080220080193.
[34] https://www.quantum-espresso.org/.
[35] P. Giannozzi, S. Baroni, N. Bonini, M. Calandra, R. Car, et al., QUANTUM ESPRESSO: a modular and open-source software project for quantumsimulations of materials, J. Phys.: Condens. Matter. 21 (2009) 395502, http://dx.doi.org/10.1088/0953-8984/21/39/395502.
[36] G. Prandini, A. Marrazzo, I.E. Castelli, N. Mounet, N. Marzari, A Standard Solid State Pseudopotentials (SSSP) Library Optimized for Accuracy and Efficiency (Version 1.0), Materials Cloud Archive, 2018, http://dx.doi.org/10.24435/materialscloud:2018.0001.
[37] K. Lejaeghere, G. Bihlmayer, T. Björkman, P. Blaha, et al., Reproducibility in density functional theory calculations of solids, Science 351 (2016) 1415, http://dx.doi.org/10.1126/science.aad3000.
[38] J.P. Perdew, K. Burke, M. Ernzerhof, Generalized gradient approximation made simple, Phys. Rev. Lett. 77 (1996) 3865, http://dx.doi.org/10.1103/PhysRevLett.77.3865.
[39] L.T. Zhuravlev, V.V. Potapov, Density of silanol groups on the surface of silica precipitated from a hydrothermal solution, Russ. J. Phys. Chem. 80 (2006) 1119, http://dx.doi.org/10.1134/S0036024406070211.
[40] D. Vogel, P. Krüger, J. Pollmann, Self-interaction and relaxation-corrected pseudopotentials for II-VI semiconductors, Phys. Rev. B 54 (1996) 5495, http://dx.doi.org/10.1103/PhysRevB.54.5495.
[41] D. Vogel, P. Krüger, J. Pollmann, Structural and electronic properties of group-III nitrides, Phys. Rev. B (1997) 12836, http://dx.doi.org/10.1103/PhysRevB.55.12836.
[42] W. Körner, C. Elsässer, First-principles density functional study of dopant elements at grain boundaries in ZnO, Phys. Rev. B 81 (2010) 085324, http://dx.doi.org/10.1103/PhysRevB.81.085324.
[43] A.D. Becke, A new mixing of Hartree–Fock and local density-functional theories, J. Chem. Phys. 98 (1993) 1372, http://dx.doi.org/10.1063/1.464304.
[44] R. Asahi, W. Mannstadt, A.J. Freeman, Optical properties and electronic structures of semiconductors with screened-exchange LDA, Phys. Rev. B 59 (1999) 7486, http://dx.doi.org/10.1103/PhysRevB.59.7486.
[45] L.G. Ferreira, M. Marques, L.K. Teles, Approximation to density functional theory for the calculation of band gaps of semiconductors, Phys. Rev. B 78 (2008) 125116, http://dx.doi.org/10.1103/PhysRevB.78.125116.
[46] A. Filippetti, N.A. Spaldin, Self-interaction-corrected pseudopotential scheme for magnetic and strongly-correlated systems, Phys. Rev. B 67 (2003) 125109, http://dx.doi.org/10.1103/PhysRevB.67.125109.
[47] G. Kresse, J. Furthmüller, Efficient iterative schemes for ab initio total-energy calculations using a plane-wave basis set, Phys. Rev. B 54 (1996) 11169, http://dx.doi.org/10.1103/PhysRevB.54.11169.

[48] G. Kresse, D. Joubert, From ultrasoft pseudopotentials to the projector augmented-wave method, Phys. Rev. B 59 (1999) 1758, http://dx.doi.org/10.1103/PhysRevB.59.1758.
[49] Ge-Qi Mao, Zhao-Yi Yan, Kan-Hao Xue, Zhengwei Ai, Shengxin Yang, Hanli Cui, Jun-Hui Yuan, Tian-Ling Ren, Xiangshui Miao, DFT-1/2 and shell DFT-1/2 methods: electronic structure calculation for semiconductors at LDA complexity, J. Phys.: Condens. Matter 34 (2022) 403001, Potential generator: see http://www.eedevice.com/vasp-half.aspx.
[50] P.E. Blöchl, Projector augmented-wave method, Phys. Rev. B 50 (1994) 17953, http://dx.doi.org/10.1103/PhysRevB.50.17953.
[51] K. Klier, J.A. Spirko, K.M. Landskron, Optical absorption anisotropy of high-density, wide-gap, high-hardness SiO2 polymorphs seifertite, stishovite, and coesite, Am. Mineral. 100 (2015) 120, http://dx.doi.org/10.2138/am-2015-4890.
[52] C. Sevik, C. Bulutay, Theoretical study of the insulating oxides and nitrides: SiO2, GeO2, Al2O3, Si3N4, and Ge3N4, J. Mater. Sci. 42 (2007) 6555, http://dx.doi.org/10.1007/s10853-007-1526-9.
[53] P. van den Keybus, W. Grevendonk, Nonresonant Faraday rotation in glassy semiconductors, Phys. Rev. B 33 (1986) 8540, http://dx.doi.org/10.1103/PhysRevB.33.8540.
[54] Z.A. Weinberg, G.W. Rubloff, E. Bassous, Transmission, photoconductivity, and the experimental band gap of thermally grown SiO2 films, Phys. Rev. B 19 (1979) 3107, http://dx.doi.org/10.1103/PhysRevB.19.3107.
[55] R. Evrard, A.N. Trukhin, Photoelectric properties and the energy gap of SiO2, Phys. Rev. B 25 (1982) 4102, http://dx.doi.org/10.1103/PhysRevB.25.4102.
[56] L.A.J. Garvie, P. Rez, J.R. Alvarez, P.R. Buseck, Interband transitions of crystalline and amorphous SiO2: An electron energy-loss spectroscopy (EELS) study of the low-loss region, Solid State Commun. 106 (1998) 303, http://dx.doi.org/10.1016/S0038-1098(98)00021-0.
[57] J. Stone, Interactions of hydrogen and deuterium with silica optical fibers: a review, J. Lightw. Technol. 5 (1987) 712, http://dx.doi.org/10.1109/JLT.1987.1075562.
[58] K. Kajihara, M. Hirano, L. Skuja, H. Hosono, Vacuum-ultraviolet absorption of interstitial O2 and H2O molecules in SiO2, J. Non-Cryst. Solids 352 (2006) 2303, http://dx.doi.org/10.1016/j.jnoncrysol.2006.02.058.
[59] K. Kajihara, T. Miura, H. Kamioka, A. Aiba, M. Uramoto, Y. Morimoto, M. Hirano, L. Skuja, H. Hosono, Diffusion and reactions of interstitial oxygen species in amorphous SiO2: A review, J. Non-Cryst. Solids 354 (2008) 224, http://dx.doi.org/10.1016/j.jnoncrysol.2007.07.038.
[60] P.V. Sushko, A.L. Shluger, The effect of the alpha-quartz lattice on the optical absorption and stretching frequency of the interstitial O2 molecule, Phys. Status Solidi 2 (2005) 503–506, http://dx.doi.org/10.1002/pssc.200460218.